ELSEVIER

Applied Surface Science 177 (2001) 158–164

applied surface science

www.elsevier.nl/locate/apsusc

Angle dependent X-ray photoemission study on UV-ozone treatments of indium tin oxide

Weijie Song[a,b], S.K. So[b], Daoyuan Wang[c], Yong Qiu[a], Lili Cao[a,*]

[a]*Department of Chemistry, Tsinghua University, Beijing 100084, China*
[b]*Department of Physics, Hong Kong Baptist University, Hong Kong, China*
[c]*ULVAC-PHI Incorporated, 370 Enzo, Chigasaki 253-0084, Japan*

Received 6 September 2000; received in revised form 15 January 2001; accepted 3 February 2001

Abstract

The surface chemistry of ITO thin-films before and after UV-ozone treatment was characterized using angle dependent X-ray photoelectron spectroscopy (ADXPS). After solvent cleaning, the ITO surface was covered with a thin nonconducting carbon contamination layer of ~7 Å. This contamination layer was removed efficiently by UV-ozone treatment, and the chemical states of the residual carbon at ITO surface after UV-ozone treatment were quite different from contaminated carbon. UV-ozone treatment modified ITO surface by introducing O^{2-} ions into ITO surface. The modified depth was about 50 Å. The modification decreased the carrier concentration at ITO surface, and thus decreased the conductivity of ITO surface.

PACS: 79.60.Dp; 81.65.Cf; 82.80.Pv

Keywords: Angle dependent X-ray photoelectron spectroscopy; Indium tin oxide; UV-ozone treatment

1. Introduction

Indium tin oxide (ITO) thin-films are widely utilized as the anode contact in light emitting diodes (OLEDs) [1,2] because these films are highly transparent and conducting. As a hole-injecting electrode, the surface properties of ITO have a direct effect on the efficiency of carrier injection into the organic layers. It is well known that surface treatments of ITO, such as UV-ozone [3] or oxygen plasma [4] treatment, can significantly improve the efficiency, brightness and reliability of OLEDs. Several investigations on modified ITO surface properties have been published [5–10]. Most of them correlated the work function of ITO and its surface chemical composition. In our previous paper [5], we discussed the removal of carbon contamination on the ITO surface using UV-ozone treatment, established a method using contact angle to show the effect of cleaning, and also examined the effects of UV-ozone treatment on OLEDs performance. Mason et al. reported that the work function of ITO is largely determined by the surface oxygen concentration [8]. Sugiyama et al. reported that three factors: (i) C-containing contaminants, (ii) the O/In ratio, and (iii) the In/Sn ratio on the ITO surface affected the work function [9]. Recently, we reported that oxygen plasma treatment could introduce oxygen to ITO surface and the surface stoichiometry was the dominant factor that controlled the

* Corresponding author. Tel.: +86-10-6278-7714.
E-mail address: cll@dns.chem.tsinghua.edu.cn (L. Cao).

0169-4332/01/$ – see front matter
PII: S0169-4332(01)00178-7

work function [10]. However, the modification details, especially the modification depth, were still not clearly known.

The analysis depth of X-ray photoelectron spectroscopy (XPS) is dependent on the photoelectron take-off angle θ. Thus, angle dependent X-ray photoelectron spectroscopy (ADXPS) is a powerful tool for nondestructive surface depth profile. This manner of depth profiling is invaluable for compositional changes that occur very close to the surface [11]. In this work, we examined the modified ITO surface properties using UV-ozone treatments employing ADXPS. Based on our results, we showed the modification details of UV-ozone treatments on ITO surface.

2. Experimental

ITO thin-films were purchased from Sanyo Vacuum Co. They have a thickness of 1500 Å and a sheet resistance of 11.4 Ω/□. Two samples were used in current experiment for comparison. ITO thin-films were first cleaned by scrubbing in detergent and then in distilled water. Then they were immersed sequentially in ultrasonic baths of ethanol and acetone, each for about 15 min. Then they were blown dry in a clean hood. One sample was then exposed to a low-pressure mercury vapor grid lamp (JELIGHT, Model 42–220) for UV-ozone treatment for 10 min. This ozone producing Hg grid lamp has a maximum emission at 253.7 nm. The radiation density is 18 000 μW/cm^2. All samples were stored in a low vacuum before analysis.

ADXPS measurements were performed using PHI Quantum 2000 System with a multi-channel detector. The base pressure of analysis chamber was better than 7×10^{-10} Torr. The XPS spectra were recorded using a monochromatic Al Kα excitation (1486.6 eV), with a power of 44.7 W and a pass energy of 58.7 eV. The diameter of X-ray spot was set to be 200 μm for small area analysis. The take-off angles (TOA, relative to sample surface) were set to be 90, 45, 15, and 5°, separately. The inelastic mean free path (λ) of photoelectron in ITO was calculated to be 23 Å according to the equation of Seah and Dench [12]. Dual neutralization was used during ADXPS analysis. In this paper, all spectra were shown without energy scale calibration.

3. Results and discussion

3.1. Atomic concentrations before and after UV-ozone treatment

The atomic concentrations before and after UV-ozonetreatments at different TOA were shown in Fig. 1. Before UV-ozone treatment, the atomic concentration

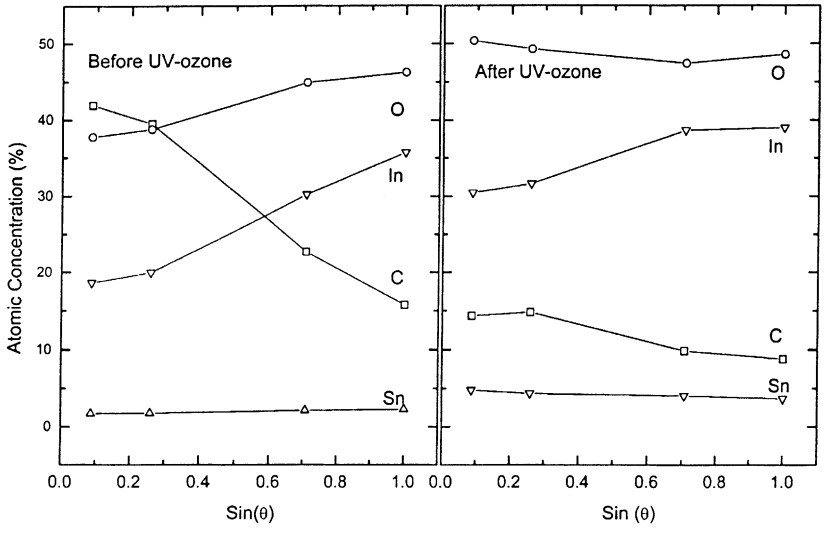

Fig. 1. The atomic concentrations of ITO surface measured at different TOA before and after UV-ozone treatment.

of carbon was about 40% at 5 and 15° TOA. It decreased quickly to about 15% when the TOA change from 15 to 90°. This indicated that there was a thin layer of carbon contamination at ITO surface after solvent cleaning. The thickness of this thin layer was less than 0.8λ. After UV-ozone treatment, the concentration of carbon decreased significantly especially at low TOA. This indicated that the carbon contamination at ITO surface was removed efficiently using UV-ozone treatment. This observation is consistent with former reports [5,8].

3.2. The XPS peaks of In 3d and the valence band spectra before and after UV-ozone treatment

The peaks of In 3d were shown in Fig. 2 and the valence band spectra were shown in Fig. 3. The highest peak in Fig. 3 should be assigned to In 4d, and the small peak located at higher binding energy should be assigned to a mixture of Sn 4d and O 2s. Comparing the peak positions of In $3d_{5/2}$ and In 4d in the valance band, it can be sure that the peak position changes at different TOA were caused by charging. Charging occurs in XPS because a nonconductive sample does not have sufficient delocalized, conduction band electrons available to neutralize the charged centers that build from clustering of the positive holes created with the photoelectron and/or Auger electron ejection [13]. It was interesting that the problem of charging arose at different TOA before and after UV-ozone treatment. Before UV-ozone treatment, charging occurred only at 5° TOA, indicating that only the top-layers (~7 Å) is nonconductive. After UV-ozone treatment, charging occurred from 45 to 5° TOA, indicating that the thickness of the nonconductive

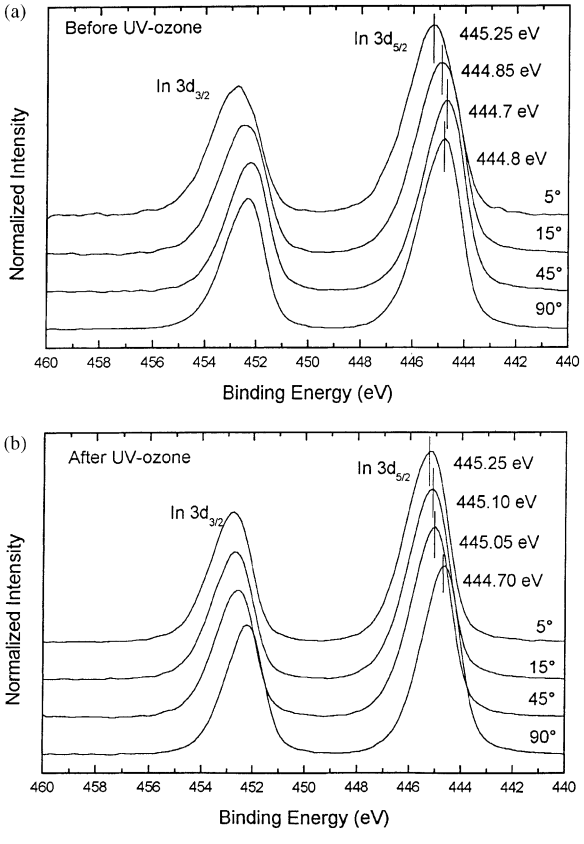

Fig. 2. The ITO core level spectra of In 3d before and after UV-ozone treatment.

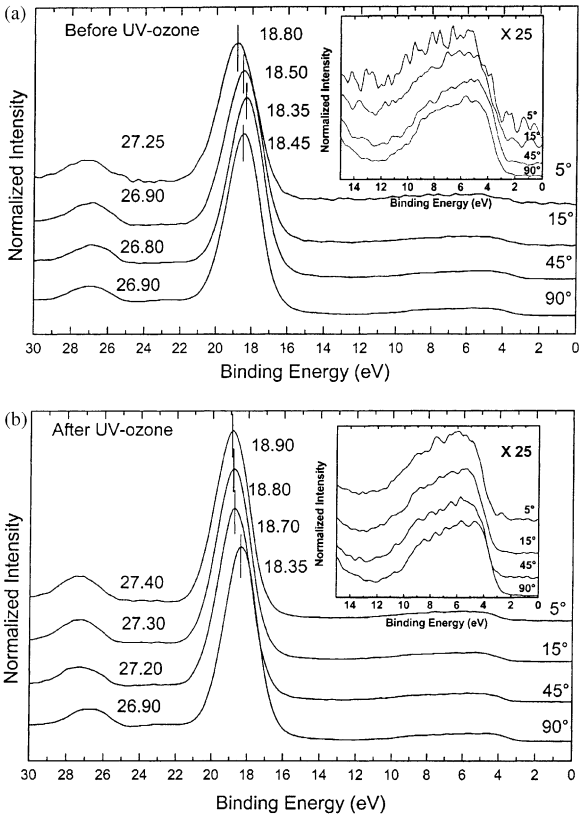

Fig. 3. The valence band spectra of ITO before and after UV-ozone treatment.

layer is about 2.1λ which is much larger than before UV-ozone treatment. Although, vertical differential charging arose during the ADXPS analysis of both before and after UV-ozone treated samples, it was actually caused by different mechanism. Before UV-ozone treatment, there was a thin layer of carbon contamination at ITO surface. The contamination is nonconductive, and thus, caused the differential charging at 5° TOA. Because the carbon contamination at ITO surface was removed efficiently after UV-ozone treatment, carbon contamination was not the origin of charging after UV-ozone treatment. Then the introduction of oxygen into ITO surface must be the cause of charging. This is reasonable because oxygen vacancy is one of the main carriers of ITO [14]. UV-ozone treatment have introduced oxygen into ITO surface, thus, the oxygen vacancies at ITO surface was decreased. This lowered the conductivity of ITO surface. It is now clear that the modification depth of ITO surface using UV-ozone treatment is about 50 Å. Since this nonconductive layer is in direct contact with the organic layers, this modification should have a direct effect on the injection of hole into organic layers.

The binding energy of In $3d_{5/2}$ were reported to be 444.7 eV both before and after oxygen plasma treatment [10]. Here, this value could be used as charge reference. UV-ozone treatment did not change the chemical state of In at ITO surface. The ITO valance band spectra from 0 to 15 eV was enlarged and shown inset Fig. 3. The band was similar to indium oxide, which was relatively flat across its entire density top with only a small (but noticeable) upward slope as one proceeds from high to low binding energy [15].

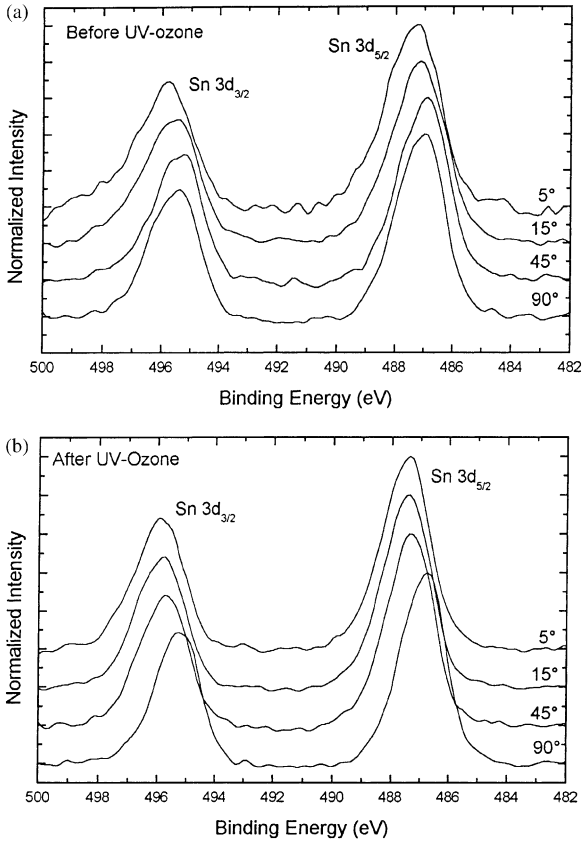

Fig. 4. The ITO core level spectra of Sn 3d before and after UV-ozone treatment.

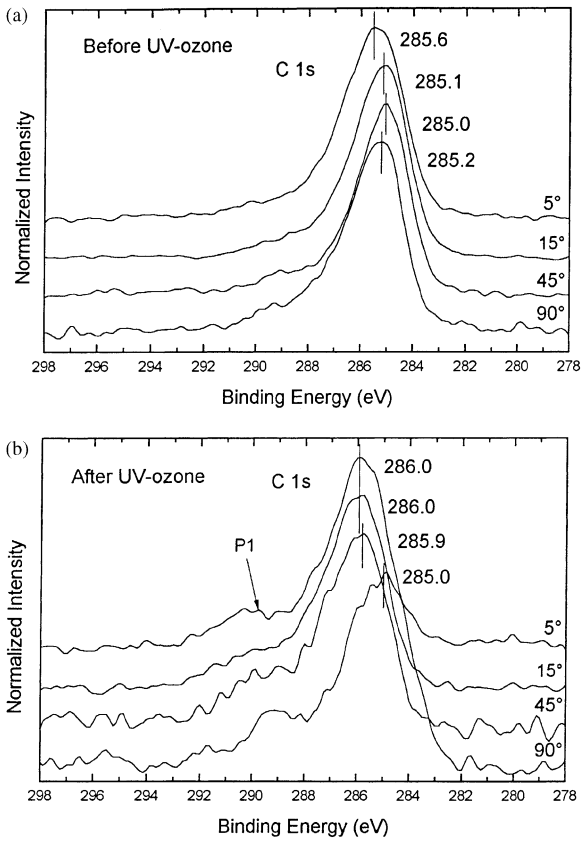

Fig. 5. The ITO core level spectra of C 1s before and after UV-ozone treatment.

A visible change was that the bandwidth was a little bit reduced when the TOA increased from 5 to 90° both before and after UV-ozone treatment. This was perhaps caused by the decrease of carbon contamination at ITO surface since the contribution of carbon contamination to the valance band was at a binding energy of about 8–10 eV.

3.3. The peak of Sn 3d before and after UV-ozone treatment

Fig. 4 showed the XPS spectra of Sn 3d before and after UV-ozone treatment at different TOA. The trend in the change of the peak position was also the same with the In 3d peak, which was caused by charging.

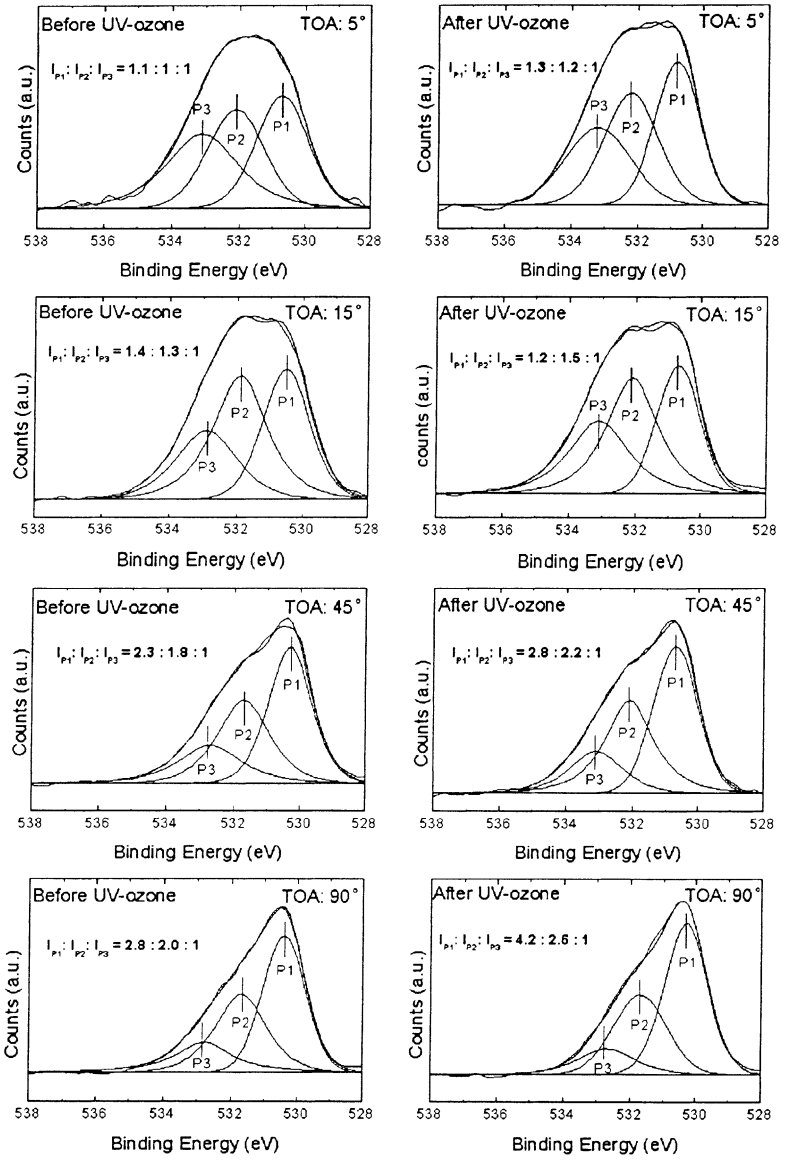

Fig. 6. The curve-fit results of O 1s ADXPS spectra before and after UV-ozone treatment.

The peak position of Sn $3d_{5/2}$ was 486.7 eV after removal the effect of vertical differential charging. This is equal to the binding energy of SnO_2 [16]. This indicated that the main component of Sn in ITO is Sn^{4+}. The peak full-width at half-maximum (FWHM) of Sn $3d_{5/2}$ at 90° TOA is about 2.00 eV, which is much higher than pure SnO_2 (about 1.30 eV in current resolution). This indicated that Sn existed in a more complex form than SnO_2 in ITO [17].

3.4. The peak of C 1s before and after UV-ozone treatment

The peaks of C 1s before and after UV-ozone treatment at different TOA were shown in Fig. 5. Before UV-ozone treatment, the peak position of C 1s was at 285.0 eV after removal the effect of vertical differential charging as described in above paragraphs. This indicated that the carbon at ITO surface is mainly hydrocarbon. After UV-ozone treatment, the C 1s peak became very complex. At 90° TOA, the peak position is at 285.0 eV, but the FWHM of C 1s main peak (2.60 eV) is larger than the peak before UV-ozone treatment (2.20 eV). It indicated that some of carbon was introduced to ITO during fabrication and could not be eliminated using UV-ozone treatment [5]. According to our experiments, prolonging treat time after 1 min can not lower the carbon at ITO surface. At 5 to 45° TOA, a wide peak (P1 as shown in Fig. 5(b)) located from 288.0 to 292.0 eV appeared after UV-ozone treatment. This peak indicated that part of hydrocarbon at ITO surface after UV-ozone treatment was oxidized into C=O, or even COO^-. The binding energy of C 1s main peak is 285.5 eV after removal the effect of vertical differential charging as described in above paragraphs, which is 0.5 eV higher than normal hydrocarbon. This should be assigned to those hydrocarbons that connected to C=O, or COO^- function groups. It can be sure that the carbon still existed at ITO surface after UV-ozone treatment is partially oxidized. Whether this partially oxidized carbon would affect the performance of OLEDs is still unknown.

3.5. The peak of O 1s before and after UV-ozone treatment

Fig. 6 showed the curve-fit results of O 1s peaks of ITO before and after UV-ozone treatment at different TOA. The O 1s peak can be fitted into three peaks. Peak 1 centered at 530.3 eV can be assigned to O^{2-} ions in the tetrahedral interstices of face-centered-cubic In^{3+} ion array [18]. Peak 3 centered at 532.8 eV is due to loosely bonded O^0 from contamination. Peak 2 centered at 531.8 eV have two contributors: (1) oxygen from C–O contamination, and (2) oxygen bonded to In and Sn in ITO; this state is the intermediate state between O^{2-} and dissociated oxygen, and its electron density is smaller than the O^{2-} ions [10]. From Fig. 6, it can be concluded that the increase of oxygen concentration should mainly be contributed to the increase of peaks 1 and 2. UV-ozone treatment not only removes the carbon contamination at ITO surface through oxidation, but also introduces O^{2-} ions into ITO surface.

4. Conclusions

The surface chemistry of ITO thin-films before and after UV-ozone treatment was investigated using ADXPS. The major results and conclusions are summarized below.

1. There was a thin layer of carbon contamination at ITO surface before UV-ozone treatment. This layer is nonconducting and the thickness is about 7 Å. UV-ozone treatment removes most of the carbon contamination at ITO surface, and the residual carbon at ITO surface is partially oxidized.
2. UV-ozone treatment can modify ITO surface through introducing O^{2-} ions into ITO surface. The modified depth is about 50 Å. The modification decreased the carrier concentration at ITO surface, thus decreased the conductivity of ITO surface.

Acknowledgements

Support of this research by the Chinese National Science Foundation #29875013 and Research Committee of Hong Kong Baptist University under Grant #FRG/98-99/II-71 is gratefully acknowledged. We would like to thank Professor Ho Wei for helpful discussions.

References

[1] C.W. Tang, S.A. Van Slyke, Appl. Phys. Lett. 51 (1987) 913.
[2] H. Kim, A. Piqué, J.S. Horwitz, H. Matloussi, H. Murata, Z.H. Kafafi, D.B. Chrisey, Appl. Phys. Lett. 74 (1999) 3444.
[3] S.A. Van Slyke, C.H. Chen, C.W. Tang, Appl. Phys. Lett. 69 (1996) 2160.
[4] C.C. Wu, C.I. Wu, J.C. Sturm, A. Kahn, Appl. Phys. Lett. 70 (1997) 1348.
[5] S.K. So, W.K. Choi, C.H. Cheng, L.M. Leung, C.F. Kwong, Appl. Phys. A 68 (1999) 477.
[6] F. Nüusch, L.J. Rothberg, E.W. Forsythe, Q.T. Le, Y. Gao, Appl. Phys. Lett. 74 (1999) 880.
[7] A. Gyoutpku, S. Hara, T. Komatsu, M. Shihama, H. Iwanaga, K. Sakanoue, Synth. Met. 91 (1997) 73.
[8] M.G. Mason, L.S. Hung, C.W. Tang, S.T. Lee, K.W. Wang, M. Wang, J. Appl. Phys. 86 (1999) 1688.
[9] K. Sugiyama, H. Ishii, Y. Ouchi, K. Seki, J. Appl. Phys. 87 (2000) 295.
[10] W. Song, S.K. So, L. Cao, Appl. Phys. A 72 (2001) 361.
[11] J.F. Watts, An Introduction to Surface Analysis by Electron Spectroscopy, Oxford University Press, Oxford, 1990, pp. 35–36.
[12] R.T. Lewis, M.A. Kelly, J. Electron Spectrosc. Rel. Phenom. 20 (1980) 105.
[13] N. Taga, H. Odaka, Y. Shigesato, I. Yasui, M. Kamei, T.E. Haynes, J. Appl. Phys. 80 (1996) 978.
[14] M.P. Seah, W.A. Dench, Surf. Inter. Anal. 1 (1979) 2.
[15] T.L. Barr, Y.L. Liu, J. Phys. Chem. Solids 50 (1989) 657.
[16] J.F. Moulder, W.F. Stickle, P.E. Sobol, K.D. Bomben, Handbook of X-Ray Photoelectron Spectroscopy, Perkin-Elmer Corporation, Eden Prairie, MN, 1992.
[17] R.B.H. Tahar, T. Ban, Y. Ohya, Y. Takahashi, J. Appl. Phys. 85 (1998) 2631.
[18] W.R. Salaneck, N. Johansson, K.Z. Xing, F. Cacialli, R.H. Friend, G. Beamson, D.T. Clark, Synth. Met. 92 (1998) 207.